ACS APPLIED MATERIALS & INTERFACES

Research Article

www.acsami.org

Silane Coupling Agent for Attaching Fusion-Bonded Epoxy to Steel

Madeleine R. Tchoquessi Diodjo,*[,†] Lénaïk Belec,[†] Emmanuel Aragon,[†] Yoann Joliff,[†] Lise Lanarde,[‡] and François-Xavier Perrin*[,‡]

[†]Laboratory MAPIEM, Université du Sud Toulon Var, Avenue Georges Pompidou - BP56, 83957, La Garde, France

[‡]GDF Suez, DRI-CRIGEN, Pôle Mécanique, Matériaux, Intégrité des structures, 361 Avenue du président Wilson, BP 33, 93211, Saint-Denis, La Plaine, France

Supporting Information

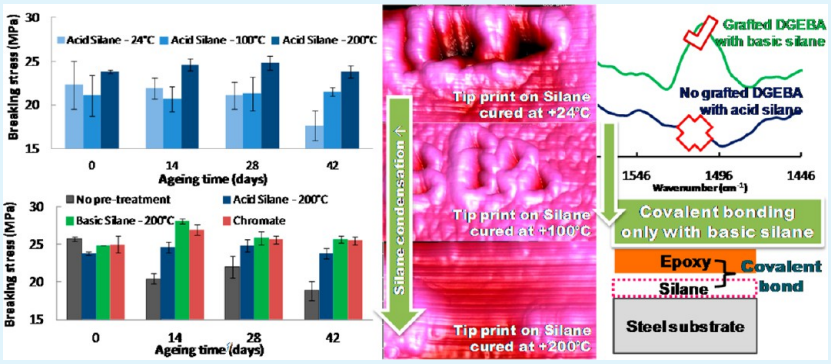

ABSTRACT: We describe the possibility of using γ-aminopropyltriethoxysilane (γ-APS) to increase the durability of epoxy powder coating/steel joints. The curing temperature of epoxy powder coatings is frequently above 200 °C, which is seen so far as a major limitation for the use of the heat-sensitive aminosilane coupling agent. Despite this limitation, we demonstrate that aminosilane is a competitive alternative to traditional chromate conversion to enhance the durability of epoxy powder coatings/steel joints. Fourier-transform reflection−absorption infrared spectroscopy (FT-RAIRS), X-ray photoelectron spectroscopy (XPS), and atomic force microscopy (AFM) were used to identify the silane deposition conditions that influence the adhesion of epoxy powder coatings on steel. We show that AFM analysis provides highly sensitive measurements of mechanical property development and, as such, the degree of condensation of the silane. The joint durability in water at 60 °C was lower when the pH of the γ-APS solution was controlled at 4.6 using formic acid, rather than that at natural pH (10.6). At the curing temperature of 220 °C, oxidation of the carbon adjacent to the amine headgroup of γ-APS gives amide species by a pseudofirst-order kinetics. However, a few amino functionalities remain to react with oxirane groups of epoxy resin and, thus, strengthen the epoxy/silane interphase. The formation of ammonium formate in the acidic silane inhibits the reaction between silane and epoxy, which consequently decreases the epoxy/silane interphase cohesion. We find that the nanoroughness of silane deposits increases with the cure temperature which is beneficial to the wet stability of the epoxy/steel joints, due to increased mechanical interlocking.

KEYWORDS: *silane coupling agent, wet adhesion, fusion-bonded epoxy, infrared spectroscopy, X-ray photoelectron spectroscopy, atomic force microscopy*

INTRODUCTION

Epoxy powder coatings are the oldest and still one of the largest classes of thermosetting powder coatings.[1] An important factor leading to their use is that volatile organic compound (VOC) emissions are very low. The powder consists of a mixture of a primary resin (bisphenol A or Novolac epoxy) and a cross-linker (polyamines or phenolics). It is generally applied to the substrate, usually metal, and fused to a continuous film by baking, at temperatures in the range of 140−240 °C. The performance of protective coatings is frequently limited by poor durability of the metal/polymer interface to wet environment.[2,3] Surface treatments based on silane coupling agents have evolved as a promising alternative for toxic chromate-based treatments because they combine several advantages like low cost, excellent corrosion protection, and adhesion properties to organic coatings such as epoxies, polyurethanes, polyesters, or acrylics.[4] γ-Aminopropyltriethoxysilane (γ-APS) carries an amino functional group which is responsible for the specific chemical reaction behavior, water solubility, and high reactivity in the self-condensation. γ-APS requires a prehydrolysis of the silane to achieve a high reactivity with the substrate to improve adhesion.[5] When the prehydrolyzed solution is applied over the metal substrate, it is generally admitted that siloxane bonds are formed through the reaction

Received: May 6, 2013
Accepted: June 21, 2013
Published: June 21, 2013

   dx.doi.org/10.1021/am401689s | ACS Appl. Mater. Interfaces 2013, 5, 6751−6761

between hydroxyl groups of the surface and the silanols.[6] At the same time, the amino group at the other end of the γ-APS molecule can create covalent bonds with polymeric coatings. The reaction between amino groups of γ-APS and epoxy is more than interfacial in nature.[7] It was then suggested that the coupling agent should not be preheated before the polymeric coating (epoxy) is added. Indeed, preheating only further condenses the coupling agent, reducing the penetration of the epoxy resin into the interphase. Moreover, a reaction temperature below 120 °C in air is preferred to limit the oxidation of the primary amines to imine groups. This explains the restrictions on the use of aminosilane with epoxy powder coatings as these silanes cannot tolerate the high temperatures required for powder coatings. Despite these limitations, it is the purpose of this paper to investigate the possibility of using aminosilanes to increase the durability of an epoxy powder coating/steel joint. The variables in silane treatment, e.g., solution concentration, solution pH, and curing conditions, strongly affect the silane bonding to the inorganic surface and the bonding between the adhesive and silane.[6−17] Thiedman et al.[14] investigated the effect of pH on the durability of aluminum joints pretreated with γ-APS and bonded with epoxy film adhesives. They observed that the joint durability increases when the pH of γ-APS solution was controlled at 8.0 rather than 10.3 using 1 M HCl. However, when 1 M phosphoric or acetic acid was used to acidify the solution, no improvement in the joint durability was obtained. They suggest that the formation of a simple amine hydrochloride would still be able to attack the epoxy rings, enabling the adhesive to react with the adsorbed silane film and improve the durability. On the contrary, phosphoric or acetic acid might react with the amino groups of γ-APS to form P−O−N bonds and amide groups, limiting the amine reactivity. Boeiro et al.[15,16] studied the effect of pH on the durability of mild steel and titanium lap shear joints pretreated with a 1% aqueous γ-APS solution. The natural pH of a 1% γ-APS solution was approximately 10.4. Then, the solutions were acidified with HCl. In the case of mild steel, they found that joints pretreated at pH 8.0 had better durability than that at pH 10.4, whereas in the case of titanium, similar durability was obtained at pH 8.0 and 10.4. Cave and Kinloch[17] also investigated the effect of the silane deposition conditions on the durability of aluminum/polyurethane joints pretreated with γ-APS using the blister test. The optimized pH of the aqueous silane solution was around 6.8. Here, we are focusing on the effect of the pH of γ-APS solution and cure temperature on the adherence and the durability of epoxy/steel joints in water. Fourier-transform reflection−absorption infrared spectroscopy (FT-RAIRS), X-ray photoelectron spectroscopy (XPS), and atomic force microscopy (AFM) were used to identify the silane deposition conditions that influence the adhesion of epoxy powder coatings on steel.

MATERIALS AND METHODS

Materials. Cold roll steel plates (E24 series) were used as a metallic substrate. The chromate solution was supplied by BASF. Fusion-bonded epoxy, aminopropyltriethoxysilane (γ-APS) aqueous solutions at pH 10.6 and pH 4.6 were provided by confidential suppliers. The γ-APS solution at pH 4.6 was prepared by adding an excess of formic acid to give a HCOOH:γ-APS molar ratio of 1.8. The γ-APS solutions were characterized by ^{1}H NMR, ^{13}C NMR, and ^{29}Si NMR spectroscopy. ^{1}H and ^{13}C NMR spectra revealed the disappearance of the peaks at 1.24 and 3.84 ppm for ^{1}H spectra and at 19 and 59.5 ppm for ^{13}C spectra, corresponding to the starting ethoxysilane, and the corresponding presence of the liberated ethanol at 1.07 and 3.55 ppm for ^{1}H and at 17.2 and 57.8 ppm for ^{13}C spectra. ^{29}Si NMR results showed that only T^i structures bearing one organic Si−R side group are observed where i refers to the number of OSi groups bound to the silicon atom of interest. Four T peaks are present, namely, T^0 (−42.37 ppm), T^1 (−50.3−51.6 ppm), T^2 (−58.0−59.1 ppm), and T^3 (−65−70 ppm). A single T^0 peak was observed which corresponds to the totally hydrolyzed γ-APS (the trisilanol, RSi-$(OH)_3$). The ^{29}Si NMR results showed that γ-APS was partially condensed even in the aqueous solution. Condensed T^1, T^2, and T^3 species were thus formed even if water solvent was expected to displace the equilibrium SiOSi + H_2O ↔ 2SiOH toward the right. The relative integrals of the Ti signals showed that the alkaline silane solution (pH 10.6) was more condensed than the acid silane solution. Tesoro and Wu[18] highlighted that for silanes such as γ-APS, γ-MPS, and γ-GPS in solution the proportion of condensation reactions was minimal for a pH value equal to 4. The above results are thus in line with literature data.

Poly(bisphenol A-co-epichlorohydrin), glycidyl end-capped (DGEBA) was used as raw material for the preparation of the different FT-IR samples (CAS number: 25036-25-3; SIGMA Aldrich). Demineralized water of 18.2 MΩ cm was used throughout this work.

Mirror polished cold roll E24 steel substrates ($R_z \cong 0.1$ μm) were used for FTIR, SEM/EDS, and XPS analyses. For single lap shear tests, E24 steel substrates were first degreased in xylene at +60 °C and then sandblasted to create a surface roughness ($R_z \cong 30$ μm), dusted with compressed air, degreased again in xylene at +60 °C, and finally air-dried. Single lap shear joints were realized according to ISO 4587 Standard. The dimensions of the steel plates used for single lap shear joints were equal to 100 × 25 × 1.5 mm^3. Four types of single lap shear joints were prepared: without silane treatment, with standard chromate conversion, and with the silane-based treatments at pH 4.6 and pH 10.6. The deposit of the silane solution was done by dipping the steel substrate during 30 s into the dilute solution followed by a 60 s air-drying. Silane was cured in air atmosphere at either 24 °C for 24 h, 100 °C for 5 min, or 200 °C for 5 min, after heating at a rate of 5 °C/min in the last two conditions. The silane films deposited from the solution at pH 4.6 and pH 10.6 were, respectively, referred to as Sil-Ac-X and Sil-Al-X, where X is the cure temperature.

A specific pressurizing tool has been implemented to prepare joints with thickness of 100 ± 15 μm. The fusion-bonded epoxy was deposited with a metallic spatula on the steel substrate. The assembly was pressurized and cured during 90 min at 220 °C.

Methods. *FTIR.* FTIR spectra were collected in reflectance mode using a Nexus 870 Thermo-Nicolet instrument coupled with a Thermo-Nicolet Continuum FTIR microscope at a 45° incidence angle. 128 scans were recorded with a resolution of 4 cm^{-1}. Each spectrum was obtained by subtracting a background spectrum obtained with the bare steel substrate. All measurements were performed at room temperature (24 ± 1 °C and 55% RH). For the study of silane/DGEBA interactions, a few millimeters thick layer of DGEBA was deposited over the precured coupling agent. Samples were cured during 2h 30 min at 130 °C. Finally, samples were maintained under agitation for 15 min with methyl ethyl ketone (MEK) to remove the unreacted epoxy resin. It has first been validated that MEK did not dissolve any of the cured polysiloxane coupling agent, yet it dissolved the unreacted heated epoxy resin from the steel substrate, indicating that no autocondensation reaction of DGEBA occurs under the above curing conditions.

XPS. XPS analysis was carried out with an XPS Scienta 200 electron spectrometer equipped with an Al monochromatic source (Al Kα energy of 1486.6 eV). High-resolution spectra were recorded at a power of 225 W. The electron emission angle was 0° for an analyzed depth lower than 10 nm. Spectra were taken by setting the instrument to the slot mode providing approximately a 300 × 700 μm^2 analysis area. The binding energy (BE) scale was corrected for static charging, using BE = 285.0 eV for the C 1s level of aliphatic hydrocarbon. Spectra were analyzed with the help of Vision processing fit program. In curve fitting, the full widths at half-maximum (fwhm's) for all component peaks were constrained to be equal. The elemental depth profiling of the silane film was acquired by material etching using

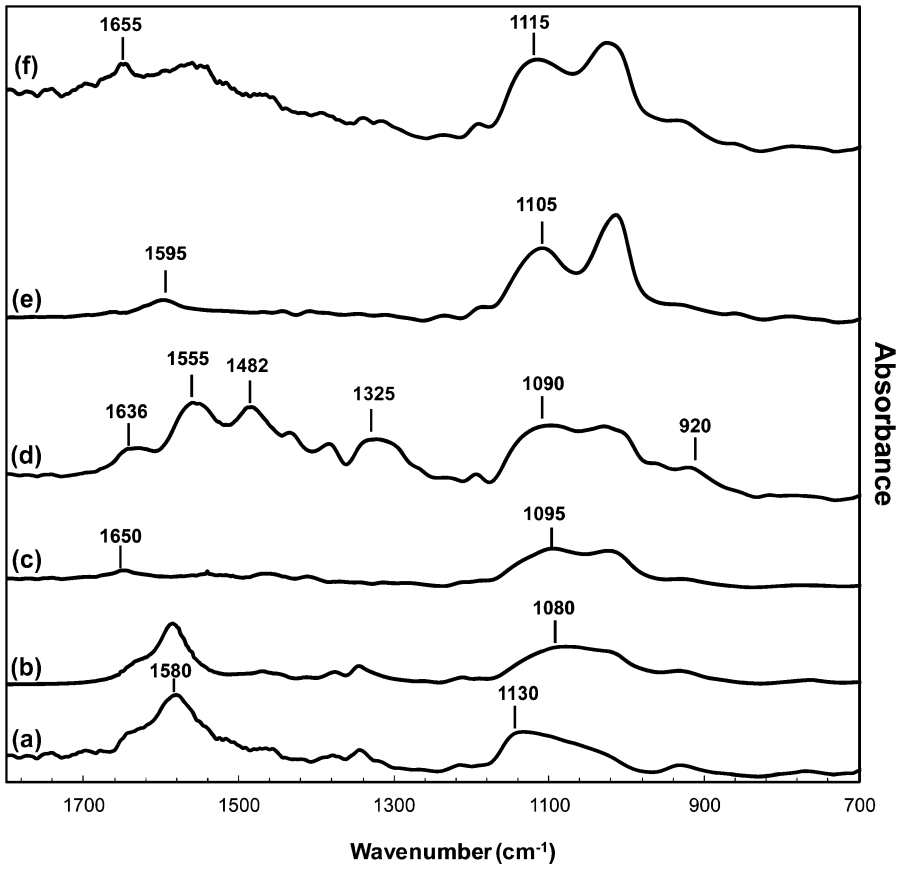

Figure 1. FTIR spectra of silane films prepared at pH 4.6 (a,b,c) and pH 10.4 (d,e,f) cured at at T = 24 °C (a,d), T = 100 °C (b,e), and T = 200 °C (c,f).

argon ion sputtering at 0.5 keV. The sputter rate for a SiO_2 film was 2.6 nm/min. Quantification with XPS was reported to be better than 10% using PET (polyethylene terephthalate) standard.

The morphology of the deposited silane was determined by a field emission scanning electron microscope (Supra 40 VP Colonne GEMINI) equipped with an energy-dispersive X-ray detector (Oxford X-max- 20). Under an accelerating voltage of 4 kV and a pressure of typically 10^{-9} mBar, EDS silicon dot mappings were obtained after 15 h of scanning associated with a time shaping of 5 μs. Images detailing morphologies were taken using an SE detector at 1200 times magnification. Each analyzed area was about 95 × 72 μm^2. The working distance is the same for all the analyzed samples and equal to 10 mm.

Atomic Force Microscopy. AFM studies were carried out using a Multimode equipped Nanoscope V from Bruker AXS with a scanner type 8610 JVLR. To minimize surface deformation and material removal, the experiments were performed in tapping mode using Bruker probes type RTESP. Topography and phase-shift images were simultaneously recorded in tapping mode at room temperature in air. Image analysis was performed on NanoScope Analysis software from Bruker. Tapping probes were used for force measurements because of their high spring constant (40−80 N/m) which emphasizes the sample deformation compared with cantilever deflection during the sample vertical displacement. The average value and standard deviation are determined from at least ten measurements.

The system sensitivity and cantilever spring constant k_c were, respectively, determined from force measurements on a rigid sample and from the thermal tune method,[19] implemented in Bruker Nanoscope (V7.3) software. Then, from the slope of the force−piezo displacement curve, it is possible to measure the stiffness of the sample k_s.[19] The measurements were performed on the approach curve between 0 and 50 nm of deflection.

In the case of a perfectly elastic tip with a spherical end and a homogeneous sample, with no adhesive effects, the Hertz model can give an estimation of Young's modulus from force measurements (eq 1).[9,20]

$$Es \cong \frac{3}{4}(1-\nu_s^2)\left(\frac{2k_s}{3}\right)^{3/2}\frac{1}{\sqrt{RF}} \quad (1)$$

where F is the maximum force applied; ν_s is the Poisson ratio of the sample (ν_s = 0.3); and R is the curvature radius of the tip (10 nm) which was estimated from force measurements on polymer samples with known modulus.

The roughness parameters (Root Mean Square (RMS) or R_q) were calculated by Analysis Software from Bruker. The average values and standard deviations were determined on five areas of 500 × 250 nm^2.

Shear Strength Tests. The tests were performed on the tensile machine Adamel Lhomargy DY35 using a 20 kN force sensor. Specimens were symmetrically positioned between the rigid supports, and a longitudinal tensile load parallel to the principal axis of the specimen was applied. One of the mechanical jaws was held stationary, while the other moves at a constant speed of 1 mm/min according to ISO 4587. Stress required to reach the break was noted. Single lap shear tests were realized at the initial time and after a hydrothermal aging in aerated demineralized water at atmospheric pressure at +60 °C during 14, 28, and 42 days. Four specimens were realized for each studied configuration.

RESULTS AND DISCUSSION

Effect of Deposition Conditions on the Structure and Morphology of Silane Films. *FTIR Spectroscopy.* FTIR spectra of silane films were determined before and after curing at 100 and 200 °C (Figure 1). Films formed at pH 10.6 show

asymmetric Si−O−Si and Si−OH stretching bands around 1100 and 920 cm^{-1}. The Si−O−Si is shifted upward from 1090 for the as-deposited film to 1105 and 1115 cm^{-1} after 100 and 200 °C curing. This is in line with a more developed siloxane network at high cure temperature.[21] Bands in the 1300−1650 cm^{-1} region are associated to the various CO_2 adsorbed species on the γ-APS-metal surface:[21,22] bidentate bicarbonate (1636 cm^{-1}), bidentate carbonate (1555 cm^{-1}), monodentate carbonate (1325 cm^{-1}), and monodentate bicarbonate (1482 cm^{-1}). An intensity decrease of the absorption bands in the 1300−1650 cm^{-1} region is observed after curing at high temperature. This confirms that the IR absorption in this region mainly arises from adsorbed CO_2 species. Heating leaves the amino group in its free NH_2 form as seen by the band at 1595 cm^{-1} characteristic of the NH_2 bending. A band at 1655 cm^{-1} appears for samples cured at 100 °C and, more evidently, after curing at 200 °C. This band has been generally ascribed to the oxidation of amine to imine.[21] Absorption in this region can also be tentatively assigned to the amide I band of primary amide. Severely oxidized aminosilane films (5 h at 220 °C) were subjected to highly humid conditions (>99% relative humidity) at 20 °C. Imines hydrolyze under these conditions to release amine (Chart 1), while amides are stable.[18,23] The intensity of the 1655 cm^{-1} band did not change after three days of exposure (Figure 1, Supporting Information). The 1655 cm^{-1} band is not related to imine but rather to amide species. This will be confirmed by XPS analysis on selected samples.

Chart 1. Formation and Hydrolysis of Imine in Aminosilane Films

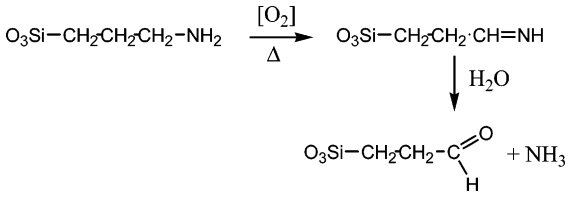

The conversion of amine to amide as a function of oxidation time at 220 °C was determined (Figure 2). The kinetics of this oxidation process fits pseudofirst-order kinetics well (shown in the inset), which suggests that the reaction proceeds under conditions of oxygen excess. A plateau is reached in the isothermal conditions (220 °C) after about 2 h. The thermal cure conditions of silane used for the preparation of the epoxy/steel assemblies gave a conversion of about 20% for the oxidation of aminopropyl to amide, leaving amino groups available to react with epoxy.

When the silane film is prepared at pH 4.6, the 1400−1650 cm^{-1} region is dominated by the band at 1590 cm^{-1} assigned to the asymmetric deformation mode of protonated amino $NH3^+$ groups of ammonium formate $HCOO^-$,$NH3^+$. The absorption due to carbonate species is insignificant. Reaction of formic acid with amino groups of γ-APS effectively prevents their reaction with atmospheric carbon dioxide. Absorption of formic acid around 1150 cm^{-1} overlaps with the Si−O−Si band. The IR spectrum found in the literature for formic acid (Aldrich FTIR handbook) displays a major characteristic peak around 1180 cm^{-1}. The release and/or partial reaction during cure at 100 °C explains the downward shift from 1130 cm^{-1} for the as-deposited film to 1080 cm^{-1}. When the silane solution is acidified with formic acid, the 1650 cm^{-1} band that appears upon heating is related to amide species. These amide species can be formed by oxidation of aminopropyl groups and by dehydration of ammonium salt on heating (Chart 2).

XPS Analysis. XPS analyses were carried out on silane-treated steel surfaces, cured at room temperature or at 200 °C. Only four elements were detected on the surfaces, namely, carbon, oxygen, silicon, and nitrogen (Table 1). Iron was not detected in all circumstances which indicated that the silane film thickness exceeds 10 nm. Thus, the contribution of the interaction between NH_2 groups and OH groups of the steel surface cannot be depicted by this analysis. After heating at 200

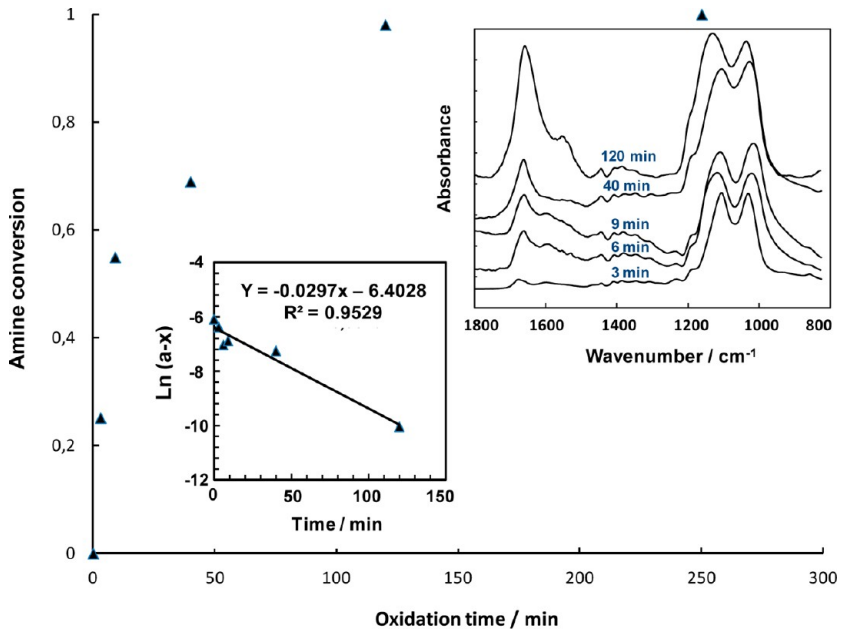

Figure 2. Conversion of amine to amide as a function of time at 220 °C for γ-APS film (pH 10.6). FTIR spectra and first-order kinetics law shown in inset.

Chart 2. Reactions of Ammonium Formate Salt on Heating in Air

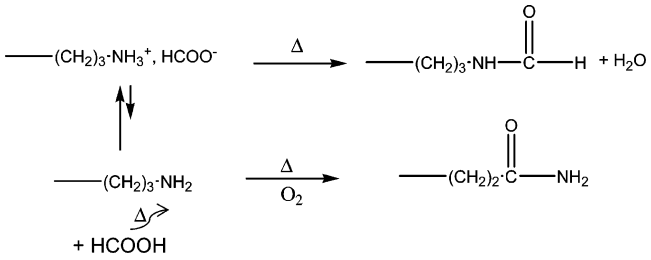

Table 1. Atomic Concentrations (Atom %) in the Silane Films Measured Using XPS

samples	O	N	C	Si
Sil-Ac-24	24.3 ± 2.4	6.9 ± 0.7	56.8 ± 5.7	12.0 ± 1.2
Sil-Al-24	23.6 ± 2.3	8.8 ± 0.9	57.9 ± 5.8	9.7 ± 1.0
Sil-Ac-200	33.2 ± 3.3	3.0 ± 0.3	60.0 ± 6.0	3.8 ± 0.4
Sil-Al-200	33.0 ± 3.0	3.8 ± 0.4	59.2 ± 5.9	4.0 ± 0.4

°C, oxygen and carbon (although to a minor extent compared to O) contents of the film increased, while the contents of Si and N decreased. Thus, the C/N ratio increases after heating. It is due to a contaminating hydrocarbon overlayer. These findings show that the silane films are easily contaminated with carbon and oxygen during or after heating in air. The increase in O content indicates that heating in air at 200 °C severely oxidizes the silane film, in agreement with FTIR findings. Figure 3 shows the elemental depth profiling of the

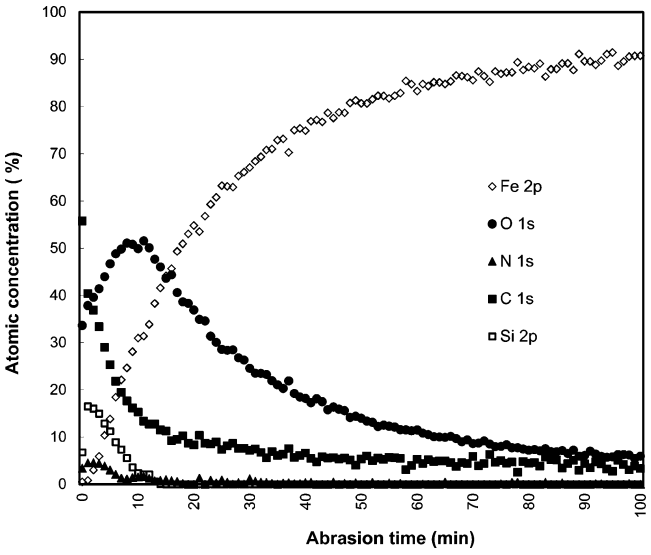

Figure 3. XPS depth analysis of the Sil-Ac-200 film.

surface layer for silane film deposited from the acid solution and cured at 200 °C. The steep decrease for C in the XPS depth profile confirms the presence of hydrocarbon contamination. From the elemental profile, it is seen that nitrogen and silicon elements follow the same thickness dependence. This suggests that the Si and N elements that are detected likely only come from the aminosilane deposit. It is thus preferred that the characteristics of the silane film be determined from the nitrogen envelope rather than from the carbon or oxygen envelopes. The silane film was about 20 nm thick (based on a 2.6 nm/min abrasion rate for SiO_2). The O 1s peak is still very strong after the first 20 nm, that is to say, when N and Si peaks have disappeared. It arises from the native iron oxide film formed in ambient atmosphere.

Figure 4 shows the high-resolution spectra of nitrogen that were peak fitted to identify functionalities present at the surface of the samples. The N 1s signal has three peaks centered at 399.1, 400.3, and 401.5 eV for all the investigated samples. The peak at 399.1 eV is assigned to the nitrogen in the free amino groups, while the peak at 401.5 eV was taken to indicate hydrogen-bonded amine or positively charged quaternary nitrogen of the form $-NH3^+$.[24] As compared to the silane film deposited from a solution at natural pH (10.6), the NH_2/$NH3^+$ atomic ratio showed a decrease by a factor of around 5 when the silane film was deposited from a solution of pH 4.6. It is related to the formation of $-NH3^+$,$HCOO^-$ ammonium carboxylate salt at acidic pH. The peak at 400.3 eV is ascribed to nitrogen in amide groups. No peak assigned to imine groups at 399 eV is identified.[25] Thus, oxidation of the carbon adjacent to the amine headgroup of γ-APS results in the formation of amide species. This reaction occurs to a minor extent after storage at room temperature but more severely upon heating in air at high temperatures.

The high-resolution C 1s spectra (Figure 2, Supporting Information) are composed of the C−SiO bond at 284.4 eV, the C−C bond at 285.0 eV, C−N at 286.3 eV (possibly superimposed by C−OR contamination), and HN−C═O and possibly C═O bonds at 287.9 eV. The amide component peak at 400.4 eV in the N 1s spectrum confirms the interpretation of the C 1s peak at 287.9 eV. After heating at 200 °C, the amide component peaks in the C 1s and N 1s spectra strongly increase, and a peak at a binding energy (BE) of 289.1 eV appears in the C 1s spectra which must result from the oxidation of the hydrocarbon contamination (CO_3 forms). Generally two chemical states of oxygen were observed in the high-resolution O 1s XP spectrum (Figure 3, Supporting Information). The high BE signal at 532.2 eV corresponds to Si−O−Si bonds and O−Si−C or O−C bonds and the low BE signal at 531 eV to O═C bonds. Expectedly, the contribution of the low BE signal strongly increased upon heating due to oxidation.

Atomic Force Microscopy. The FESEM images and EDS silicon mapping results indicate that the silane film prepared at pH 4.6 is overall homogeneous on the micrometric length scale (Figure 4, Supporting Information). More information on the nanolevel dispersion is expected from AFM analysis. The height and phase contrast AFM images of the room-temperature sample show formation of islands with diameters in the range of 70−200 nm and with a few tens of nanometers height (Figure 5). The height of the islands confirms that multilayer structures are created from the condensation between silane molecules since the expected height of a γ-APS monolayer is about 0.7 nm.[26]

These islands give rise to a high phase shift (A), while the surrounding areas correspond to medium phase shift values (B) where the silane film is probably thinner. The phase shift is related to local energy dissipation on the surface due to tip−sample inelastic processes.[27] It can be attributed to the film viscoelastic properties and/or to interactions between the probe tip and surface functional groups. The hysteresis between the approach and retract curve decreases with phase shift, revealing a high viscoelastic and/or adhesive behavior in A and a more elastic response in B. Moreover, modulus values, as

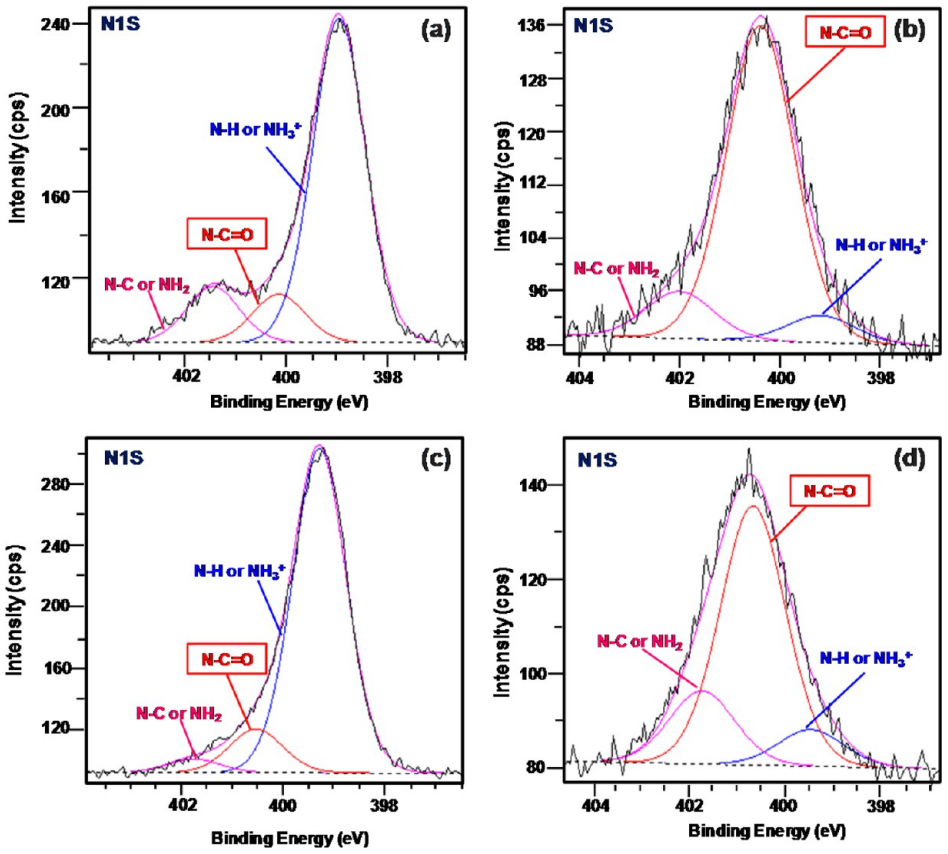

Figure 4. High-resolution N 1s photoelectron spectra for the silane films deposited from acid (a, b) and basic (c,d) solutions and cured at 24 °C (a,c) and 200 °C (b,d).

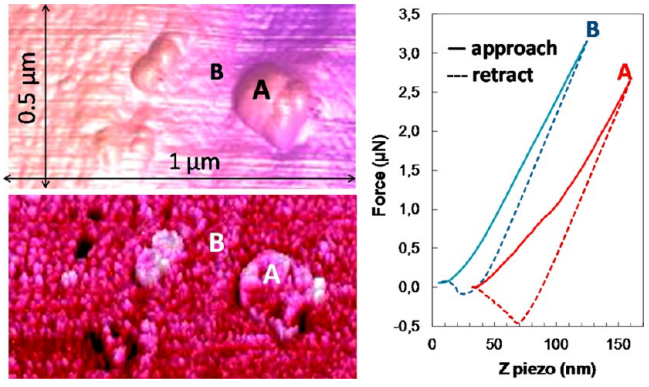

Figure 5. Silane film prepared at pH = 4.6 and cured at 24 °C AFM height image (top left, Z-scale of 300 nm) and phase image (bottom left, Z-scale of 50) on 1 μm × 0.5 μm and force curves on locations A and B (right).

calculated from eq 1 on approach curves, increase from 650 MPa on islands A up to 2.5 GPa on areas B. We made the assumption that the silane thickness was smaller in areas B than in areas A which resulted in a larger contribution of the metal substrate to the whole mechanical response in areas B.

Contrary to the data on the silane prepared in acidic conditions, large aggregates with a size in the micrometer scale are visible in the SEM images of the film prepared at pH 10.6 (Figure 4, Supporting Information). The height scans confirm the alkaline silane film heterogeneities with the identification of isolated islands of a few hundred nanometers height/width and island aggregates, identified by SEM, of a few micrometers width (Figure 6). We performed dynamic light scattering (DLS) measurements of the precursor solutions and found that aggregates in the submicrometer size range are formed at pH 4.6, while aggregates with a broader distribution and larger sizes (from few tens of nanometers to few micrometers) are formed at pH 10.6. Thus, it can be inferred that the island formation results from silane aggregates previously formed in the solution, as proposed in a previous work.[28] Force curves on different locations, on top of island aggregates, or isolated island or on thinner areas show similar mechanical behaviors with a high hysteresis between approach and retract curves. The elastic moduli are calculated on the linear range of the approach curves which are superimposed up to 3.5 μN. An average elastic modulus around 250 MPa was measured (with a deviation lower than 10%) on 10 different locations. The reproducibility as well as the value eliminate a potential contribution of the metal substrate from the mechanical response, which is also confirmed by the approach curve linearity up to very high force. All these results suggest that the silane film at pH 10.6 is thicker than the film prepared at pH 4.6. The apparent elastic modulus of the silane film prepared at pH 4.6 is higher than the values found at pH 10.6 which might indicate that a more cross-linked network was obtained at pH 4.6. The silanol self-condensation can be monitored by the decrease of the SiOH vibration around 920 cm^{-1} (Figure 5, Supporting Information). The fraction of unreacted silanol appears higher at pH 4.6 than at pH 10.6 which is in line with faster condensation kinetics in alkaline conditions. We infer that the high apparent modulus values found at pH 4.6 are due to a contribution of the metal substrate to the whole mechanical response.

dx.doi.org/10.1021/am401689s | ACS Appl. Mater. Interfaces 2013, 5, 6751−6761

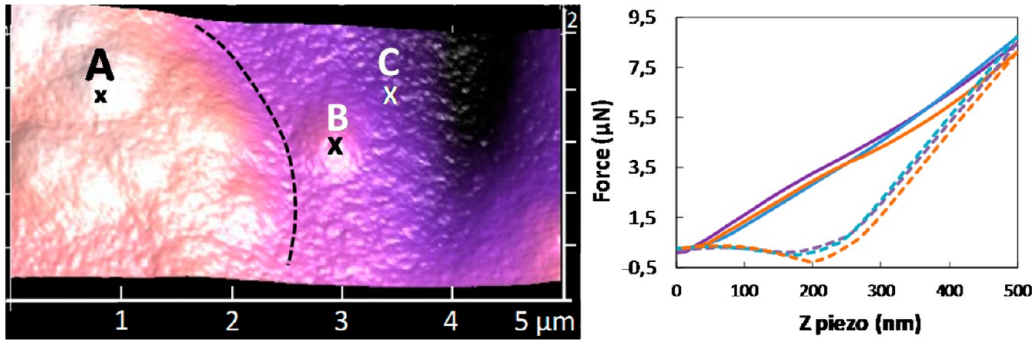

Figure 6. AFM height image (top) on silane prepared at pH = 10.6 and cured at 24 °C on 5 μm × 2.5 μm (Z-scale of 700 nm) and force curves on three different locations: (A) portion of island agglomerates, (B) isolated island, and (C) out of island area (bottom).

The characterization of the acid silane film mechanical properties by AFM is controversial due to the contribution of the steel substrate to the whole mechanical response. Then, only topography and phase images were taken into account to bring out the effects of the cure temperature on the acid silane film.

Figures 7 and 8 show that the curing temperature has a significant influence on the films' surface morphology. The

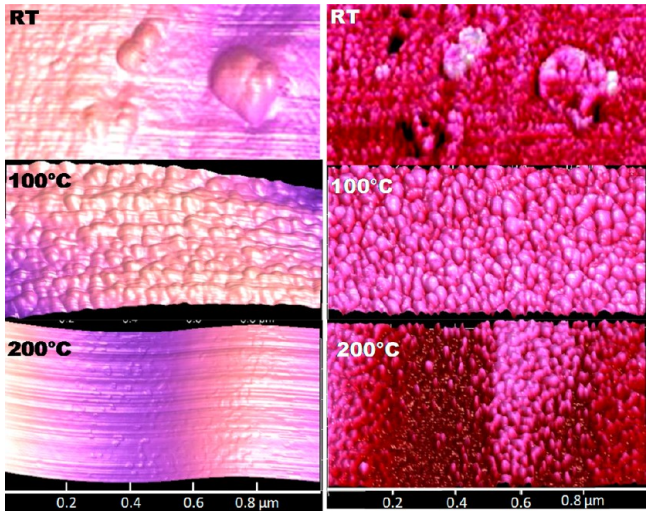

Figure 7. AFM height image (left) and phase image (right) on 1 μm × 0.5 μm (Z-scale of 100 nm) of silane film prepared at pH = 4.6 and cured at 24, 100, or 200 °C.

treatment at 100 °C homogenizes the film prepared at pH 4.6, which shows regular domains of several tens of nanometers width, associated with high phase contrasts. These domains are no longer visible on the height scan after the treatment at 200 °C, and they appear much smaller and irregularly on the phase contrast image. This evolution can be explained by the increasing condensation of the silane network, as observed from FTIR analysis, which amplifies the elastic response at 200 °C.

AFM images of the as-deposited silane film prepared at pH 10.6 displayed at the same scale as those at pH 4.6 are different from the acid one (Figure 8). They show domains of a few tens of nanometers width and around 10 nm height (i.e., a mean number of γ-APS layers around 14), associated with a high phase contrast, whatever the considered area (island or depressed area). The domain size and phase shift decrease with increasing curing temperature. Like in the case of acid

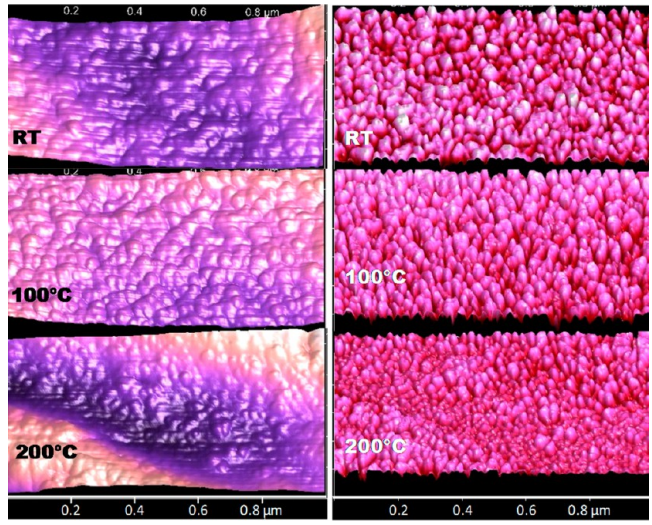

Figure 8. AFM height image (left) and phase image (right) on 1 μm × 0.5 μm (Z-scale of 100 nm) of silane film prepared at pH = 10.6 and cured at 24, 100, or 200 °C.

silane, the drop-off in energy dissipation can be correlated with the increasing silane condensation with curing temperature. The roughness data collected by AFM (Figure 9) give a more quantitative picture of the morphological changes observed in AFM images. No difference in roughness can be observed after curing at room temperature or 100 °C, on either alkaline or

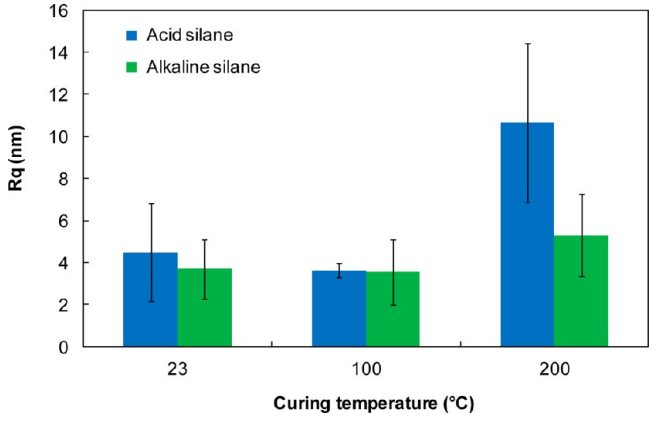

Figure 9. Root mean square roughness (R_q) for silane films cured at 24, 100, or 200 °C.

dx.doi.org/10.1021/am401689s | ACS Appl. Mater. Interfaces 2013, 5, 6751−6761

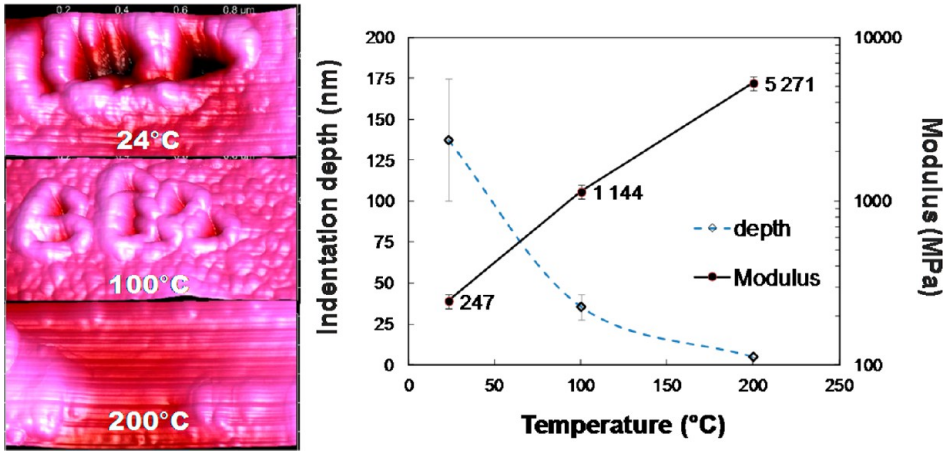

Figure 10. Tip prints after force measurements on silane films prepared at pH = 10.6 after curing at 24, 100, and 200 °C, on AFM height scans of 1 × 0.5 × 0.2 μm^3 (left) and evolution of indentation depth after force measurements and surface elastic modulus (error bars of around 10% on each modulus value) (right).

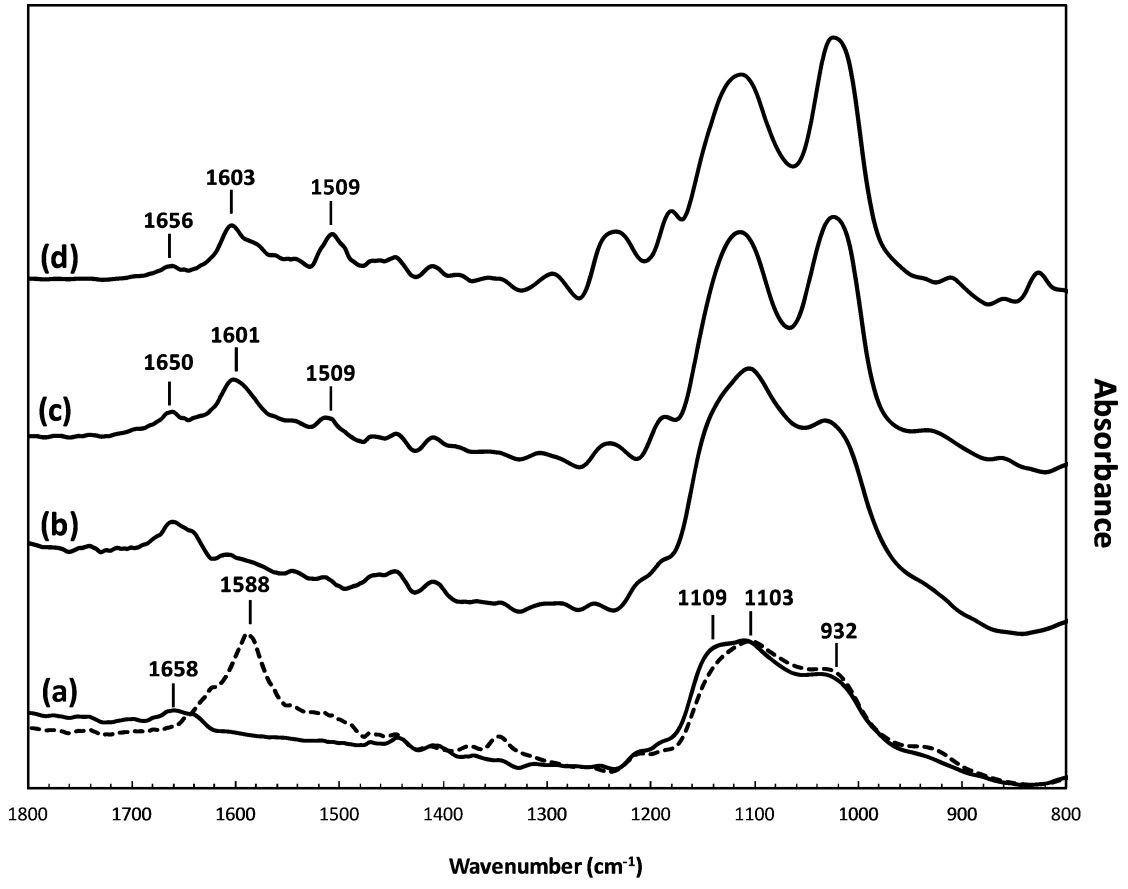

Figure 11. FTIR spectra of silane films prepared at pH 4.6 (a,b) and pH 10.4 (c,d) and cured at T = 100 °C (a,c) or T = 200 °C (b,d) after contacting with DGEBA. The dashed curve corresponds to the FTIR spectrum of silane film prepared at pH 4.6 and cured at T = 100 °C, before contacting with DGEBA.

acid silane, while a high increase in roughness appears after curing at 200 °C, especially on the acid silane film.

To confirm the evolutions observed by AFM in scanning mode, the mechanical properties of silane films at pH 10.6 were characterized by local force measurements at each temperature. A hysteresis is systematically observed between approach and retract curves after curing at room temperature or 100 °C (Figure 6, Supporting Information). This behavior reflects energy dissipation by plastic, viscous, or adhesive effects.[27] The linearity of the approach curves as well as the higher slope of the retract curves suggest viscous and/or adhesion phenomena on the tip rather than plastic effects. The highest dissipation is observed on the silane film cured at room temperature, while it is no longer detectable at 200 °C where the film behavior is elastic. At low curing temperature, a large amount of unreacted silane will enhance the viscous response and adhesive

phenomena with the tip. On the opposite, at 200 °C, the silane network is highly condensed and then responds in an elastic manner without adhesive effects.

The increase in silane network condensation with increasing temperature could also explain the evolution of tip prints after force measurements. The scans were performed a few minutes after the successive measurements. The indentation depth as well as the surrounding material throw-up decrease with increasing curing temperature (Figure 10). The less condensed silane network will generate strong viscous and adhesive effects on the tip, as suggested by approach−retract curves, leading to a large deformation of the film. The elastic modulus (as calculated from eq 1) was measured on different locations of each silane film, on the approach curve, and in the same force range (Figure 10). The values hugely increase from a few hundred MPa up to 5 GPa between the curing at room temperature and at 200 °C, respectively, which confirms the increasing condensation of the silane film with curing temperature. The highest modulus of 5 GPa is in the same range as the modulus values found for an alkaline γ-APS films deposited on steel[29] or epoxysilane/aminosilane[30] coatings.

FTIR analysis (Figure 5, Supporting Information) indicates that a full cross-linking is clearly not reached after curing at 100 °C at pH 4.6, while the situation is less obvious at pH 10.6.

Altogether, these results reveal that AFM analysis provides highly sensitive measurements of mechanical property development (and as such, the cure state), while FTIR analysis is less sensitive to changes occurring at the later stage of silane network development.

Silane Epoxy Interphase Chemistry. The commonly accepted mechanism for the enhancement of the adhesion of organic species by silane deposition is explained by interfacial coupling.[21] γ-APS contains alkoxysilane groups that can react with the steel substrate at one end and amine groups that react with the organic coating at the other end. It was found that the silane film on steel was not displaced by MEK, suggesting a strong metal−silane interaction. The covalent bridging links between epoxy resin and γ-APS were studied by depositing a thick DGEBA film over a precured coupling agent.

Figure 11 shows the IR spectra of silane treatment after its contact with epoxy resin. With the 100 °C cured silane prepared at pH 4.6, a small positive shift of the Si−O−Si band from 1103 to 1109 cm^{-1} and a decrease in the intensity of the Si−OH band around 932 cm^{-1} are observed. This shows that the silane interphase is further condensed when contacted with DGEBA at 130 °C. Other changes are the formation of a band at 1658 cm^{-1}, while the 1588 cm^{-1} band vanishes completely. The 1658 cm^{-1} band is related to the amide I band of amides, as discussed before. The band due to the phenyl rings of DGEBA at 1500 cm^{-1} can be used to determine the amount of DGEBA resistant to the MEK wash. The lack of the 1500 cm^{-1} band in all IR spectra of silane films prepared at pH 4.6 shows that DGEBA is not chemically grafted to aminosilane. This could be explained by considering that the oxidation of aminopropyl and dehydration of ammonium salt are competitive with amino-oxirane reaction.

Contrary to the acid silane treatment, a significant amount of epoxy resin is left in the siloxane interphase prepared at pH 10.6, as revealed by the aromatic band at 1509 cm^{-1}. DGEBA is also clearly grafted on the silane cured at 200 °C. The band near 1600 cm^{-1} may be related to the NH_2 deformation mode of residual amino groups and aromatic skeletal vibration of grafted DGEBA.[31] Therefore, the amine of the coupling agent stays reactive toward the epoxy resin for the silane films deposited from the natural pH (10.6) solution. Figure 12 shows

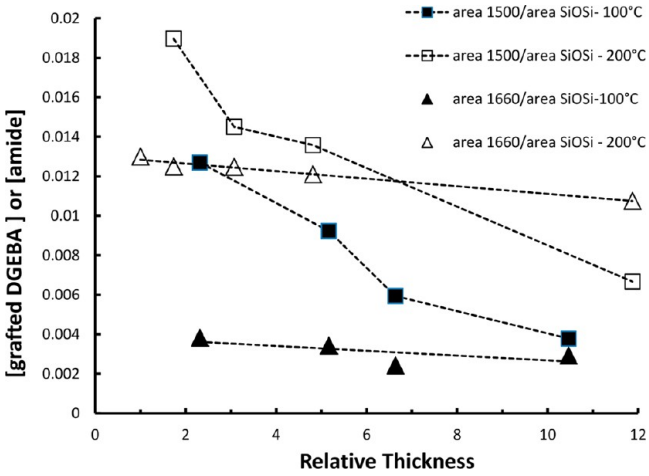

Figure 12. Concentration of grafted DGEBA and amide versus relative thickness of the silane film treated at 100 or 200 °C. Bolded lines are drawn as a guide to the eye.

the concentration of grafted DGEBA and amide species determined from FTIR analysis in areas of different thickness. The apparent concentration of grafted DGEBA clearly decreases as the thickness of silane film increases, while the amide concentration remains nearly constant regardless of the film thickness. These findings suggest that DGEBA/γ-APS reaction becomes limited by diffusion above a critical thickness, while transport limitations are not operative for the oxidative process of amine conversion to amide.

Factors Influencing Dry and Wet Adhesion. The single lap shear test data plotted in Figure 13 illustrate the influence of the curing conditions of the silane pretreatment on the durability of fusion-bonded epoxy/steel joints. It is generally assumed that the silanes should not be preheated before the epoxy resin is added. First, preheating further condenses the silane, reducing the penetration of the resin into the coupling agent interphase. Second, preheating γ-APS above 115 °C in air will oxidize amine groups, decreasing its reactivity with the epoxy resin.[21] The results revealed that surface treatments have little effect on the adhesion of coating to the steel substrate in dry conditions. However, surface treatments substantially enhanced the adhesion strength in the wet stage. It is notable that, contrary to the initial expectations, the best wet adhesion strengths are obtained when the silane layer is precured at 200 °C (Figure 13a). In light of AFM results, it is believed that the change in morphology with cure temperature is responsible for this unexpected finding. We presume that the nanoroughness evolution (Figure 9) can be correlated to the mechanical anchorage of the epoxy in the silane layer. The greater roughness of the silane film cured at 200 °C results in greater mechanical interlocking of the epoxy and, consequently, stronger adherence under dry and wet conditions compared to silane cured at room temperature or 100 °C. As shown from FTIR and XPS analysis, the poor wet adherence of the silane precured at room temperature can also be explained by the presence of ammonium salts at the silane surface. The adhesion enhancement of the joints when the silane is cured at a high temperature suggests that the decomposition of ammonium formate salts on heating should be preferably realized before

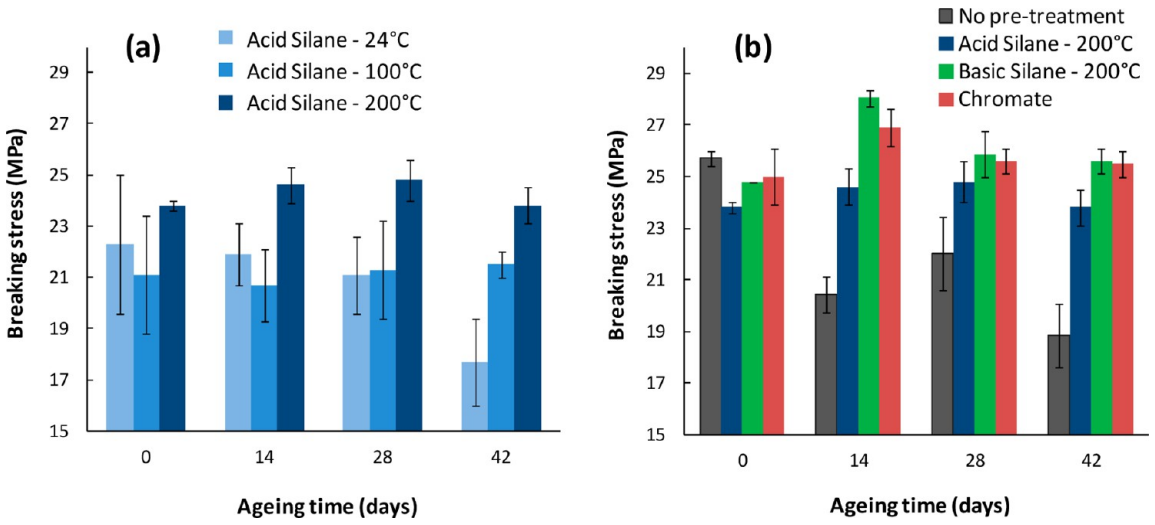

Figure 13. Influence of the cure temperature of the acid silane pretreatment (a) and silane pH (b) on wet adherence of epoxy joints during immersion at 60 °C.

contacting the silane-treated metal with the organic resin. Indeed, during epoxy application at 220 °C, the release of these species at the epoxy/silane interphase may create microflaws which increase water diffusion paths. Besides, Figure 13b shows a lower adherence of acid silane in comparison to basic silane. This seems in disagreement with other previous studies[32,33] which revealed a better adhesion performance when deposition was carried out from a low pH silane solution rather than a high pH solution. It was suggested that when the treating bath pH is below the isoelectric point (IEP) of the substrate the metal surface becomes positive and repels the amine, causing "right-side-up" orientation. Above the IEP, the amine tends to orient toward the negatively charged metal surface. This bonding arrangement is highly susceptible to hydrolysis in the presence of water. Our results show that the effect of pH of the silane solution on the orientation of γ-APS is not the decisive factor that controls the wet durability of the adhesive joints. This unusual adhesion behavior can be related to the formation of a bridge across the silane/organic resin interface at pH 10.6, as revealed by FTIR analysis. At pH 10.6, XPS and FTIR results revealed a partial oxidation of the carbon adjacent to the amine headgroup of γ-APS to give amide species. However, a few amino functionalities remain to react with oxirane groups of epoxy resin and, thus, strengthen the epoxy/silane interphase. On the contrary, at pH 4.6, formic acid reacts with amino groups of silanes to give amides, severely limiting its reaction with epoxy. It is noteworthy that the basic silane cured at 200 °C has better durability than the joint prepared with acid silane, even though basic silane deposit is less rough than acid silane. This suggests that the chemical bonding between silane and FBE is a more decisive factor than the roughness of silane deposit to increase the wet durability of silane−FBE assemblies. It must be pointed out that the performance of the silane treatment at its natural pH is comparable to standard chromate conversion which opens up the possibility for a more environmentally friendly manufacturing process for durable epoxy powder coatings/metal assemblies.

CONCLUSIONS

We find that the silane coupling agent can strongly improve the wet durability of the fusion-bonded epoxy (FBE) joints that are prepared at high temperatures (around 200 °C). This is an important result since it is generally accepted that aminosilane must not be cured at high temperatures to limit the oxidation of amine functionalities. Thus, it might have been expected that aminosilanes are not appropriate coupling agents for FBE joints typically prepared around 200 °C. Instead, we find that preheating the silane prepared in acidic conditions (pH 4.6) at a high temperature (200 °C) increases the roughness of the silane deposit and consequently the mechanical interlocking between silane and epoxy. The joints pretreated at pH 10.6 had better durability than at pH 4.6. This was related to the formation of a bridge across the silane/organic resin interface at pH 10.6, whereas at pH 4.6, the formation of ammonium formate severely limits the reaction between silane and epoxy. At pH 10.6, XPS and FTIR results revealed a partial oxidation of the carbon adjacent to the amine headgroup of γ-APS to give amide species. However, a few amino functionalities remain to react with oxirane groups of epoxy resin and strengthen the epoxy/silane interphase. Another important result is that aminosilane treatments at pH 4.6 also improved the wet durability of FBE joints, which means that a strong interfacial coupling between the organic resin and silane is not a prerequisite for the enhancement of the adhesion performance of joints by organosilane. This result is not surprising since silanes with organic groups that are not able to react with the resin were found to be effective adhesion promoters.[19]

ASSOCIATED CONTENT

Supporting Information

Six additional figures; FTIR spectra of deposited acid silane films cured at 200 °C for 5 h before and after exposure to >99% relative humidity for 3 days; high-resolution C 1s and O 1s photoelectron spectra for the acid and alkaline silane films cured in various conditions; FE-SEM images and EDS silicon dot mappings for the silane film cured at 200 °C; FTIR spectra of silane films cured at different temperatures; and AFM typical force curves for the alkaline silane films cured at different temperatures. This material is available free of charge via the Internet at http://pubs.acs.org.

AUTHOR INFORMATION

Corresponding Author

*E-mail: perrin@univ-tln.fr; tchoques@univ-tln.fr.

Author Contributions

The manuscript was written through contributions of all authors. All authors have given approval to the final version of the manuscript.

Notes

The authors declare no competing financial interest.

■ ACKNOWLEDGMENTS

The authors acknowledge Michel Meyer and Melissandre Bonnaudet from GDF for their support and expertise. GRTgaz, especially Carole de Charentenay and Philippe Merrien, are acknowledged for the financial support.

■ ABBREVIATIONS

γ-APS, γ-aminopropyltriethoxysilane
FTIR, Fourier-transform infrared spectroscopy
XPS, X-ray photoelectron spectroscopy
BE, binding energy
AFM, atomic force microscopy
NMR, nuclear magnetic resonance
VOC, volatile organic compound
DGEBA, bisphenol A diglycidyl ether
MEK, methyl ethyl ketone
IEP, isoelectric point
SEM/EDS, scanning electron microscopy with X-ray micro-analysis
FE-SEM, field emission scanning electron microscopy

■ REFERENCES

(1) Misev, T. E. In *Powder Coatings Chemistry and Technology*; Wiley-interscience: New York, 1991; p 113.
(2) Kinloch, A. J.; Gledhill, R. A. *J. Adhes.* **1974**, *6*, 313−319.
(3) Legghe, E.; Aragon, E.; Bélec, L.; Margaillan, A.; Melot, D. *Prog. Org. Coat.* **2009**, *66*, 276−280.
(4) Pluddemann, E. P. In *Silane Coupling Agents*, 2nd ed.; Plenum Press: New York, 1991.
(5) Suzuki, N.; Ishida, H. *Macromol. Symp.* **1996**, *108*, 19−53.
(6) Jussila, P.; Ali-löytty, H.; Lahtonen, K.; Hirsimäki, M.; Valden, M. *Surf. Interface Anal.* **2010**, *42*, 157−164.
(7) Culler, S. R.; Naviroj, S.; Ishida, H.; Koenig, J. L. *J. Colloid Interface Sci.* **1986**, *109*, 69−79.
(8) Ishida, H. *Polym. Compos.* **1984**, *5*, 101−123.
(9) Ondrus, D. J.; Boerio, F. J. *J. Colloid Interface Sci.* **1988**, *124* (no1), 349−357.
(10) Ondrus, D. J.; Boerio, F. J. *J. Colloid Interface Sci.* **1990**, *139* (no 2), 446−456.
(11) Davis, S. J.; Watts, J. F. *Int. J. Adhes. Adhes.* **1996**, *16*, 5−15.
(12) George, I.; Viel, P.; Bureau, C.; Suski, J.; Lécayon, G. *Surf. Interface Anal.* **1996**, *24*, 774−780.
(13) Quinton, J.; Thomsen, L.; Dastoor, P. *Surf. Interface Anal.* **1997**, *25*, 931−936.
(14) Thiedman, W.; Tolan, F. C.; Pearce, P. J.; Morris, C. E. M. *J. Adhes.* **1987**, *22*, 197−210.
(15) Ondrus, D. J.; Boerio, F. J.; Granen, K. J. *J. Adhes.* **1989**, *29*, 27−37.
(16) Boerio, F. J.; Gosselin, C. A.; Dillingham, R. G.; Lin, H. W. *J. Adhes.* **1981**, *13*, 159−176.
(17) Cave, N. G.; Kinloch, A. J. *J. Adhes.* **1991**, *34*, 175−187.
(18) Tesoro, G.; Wu, Y. *J. Adhes. Sci.Technol.* **1991**, *5*, 771−784.
(19) Hutter, J. L.; Bechhoefer, J. R. *Sci. Instrum.* **1993**, *64*, 1868−1873.
(20) Butt, H.-J.; Cappella, B.; Kappl, M. *Surf. Sci. Rep.* **2005**, *59*, 1−152.
(21) Culler, S.; Naviroj, S.; Ishida, H.; Koenig, J. *J. Colloid Interface Sci.* **1983**, *96*, 69−79.
(22) Roche, V.; Perrin, F. X.; Gigmes, D.; Vacandio, F.; Ziarelli, F.; Bertin, D. *Thin Solid Films* **2010**, *518*, 3640−3645.
(23) Suzuki, K.; Matsu-Ura, N.; Horii, H.; Sugita, Y.; Sanda, F.; Endo, T. *J. Polym. Sci., Part A: Polym. Chem.* **2002**, *40*, 971−975.
(24) Huang, N.; Michel, R.; Voros, J.; Textor, M.; Hofer, R.; Rossi, A.; Elbert, D. L.; Hubbell, J. A.; Spencer, N. D. *Langmuir* **2001**, 489−498.
(25) Luo, Y.; Bernien, M.; Krüger, A.; Hermanns, C. F.; Miguel, J.; Chang, Y.-M.; Jaekel, S.; Kuch, W.; Haag, R. *Langmuir* **2012**, *28*, 358−366.
(26) Heiney, P. A.; Grüneberg, K.; Fang, J. *Langmuir* **2000**, *16*, 2651−2657.
(27) Cleveland, J. P.; Anczykowski, B.; Schmid, a. E.; Elings, V. B. *Appl. Phys. Lett.* **1998**, *72*, 2613.
(28) Vandenberg, E. T.; Bertilsson, L.; Liedberg, B.; Uvdal, K.; Erlandsson, R.; Elwing, H.; Lundstrom, I. *J. Colloid Interface Sci.* **1991**, *147*, 103−118.
(29) Bouchet, J.; Pax, G. M.; Leterrier, Y.; Michaud, V.; Manson, J.-A. E. *Compos. Interfaces* **2006**, *13*, 573−588.
(30) Bascom, W. D. *Composite Materials*; Academic Press: New York, 1974; Vol. *6*, chap 2.
(31) Culler, S. R.; Ishida, H.; Koenig, J. L. *Polym. Compos.* **1986**, *7*, 231−238.
(32) Mohseni, M.; Mirabedini, M.; Hashemi, M.; Thompson, G. E. *Prog. Org. Coat.* **2006**, *57*, 307−313.
(33) Ooij, V.; Sabata, J. *J. Adhes. Sci. Technol.* **1991**, *5*, 843−863.